SAND2019-0077C

First Neutron Edge-Illumination (Structured Illumination) Imaging at Oak Ridge National Laboratory CG-1D Beamline

Michael D. Vincent[1, a], Kyungmin Ham[1,b] Wieslaw J. Stryjewski[1,c], Warren W. Johnson[2,d], Leslie G. Butler[3,e], Amber L. Dagel[4,f], R. Derek West[4,g], Joachim Schulz[5,h], Christian Gruenzweig[6,i], Jean C. Bilheux[7,j], Matthew R. Pearson[7,k], W. Barton Bailey[7,l], and Hassina Z. Bilheux[7,m]

[1]CAMD, LSU, Baton Rouge, LA, USA [2]Dept. of Physics & Astronomy, LSU, Baton Rouge, LA, USA [3]Dept. of Chemistry, LSU, Baton Rouge, LA, USA [4]Sandia National Laboratories, Albuquerque, NM USA [5]Karlsruhe Institute of Technology, Karlsruhe, Germany [6]Paul Scherrer Institute, Laboratory for Neutron Scattering and Imaging, Villigen, Switzerland [7]Oak Ridge National Laboratory, Oak Ridge, TN, USA

[a]mvinc15@lsu.edu, [b]kham1@lsu.edu, [c]w.j.stryj@s2gllc.com, [d]warren.johnson@phys.lsu.edu, [e]lbutler@lsu.edu, [f]aldagel@sandia.gov, [g]rdwest@sandia.gov, [h]joachim.schulz@kit.de, [i]christian.gruenzweig@psi.ch, [j]bilheuxjm@ornl.gov, [k]pearsonmr@ornl.gov, [l]baileywb@ornl.gov, [m]bilheuxhn@ornl.gov

Keywords: grating-based interferometry, edge-illumination, structured illumination, neutron imaging

Abstract: A mask-stepping imaging method, developed for X-ray phase contrast imaging by A. Olivo and co-workers, has been adapted for neutron imaging. In this preliminary experiment, initial results show both phase contrast and scatter imaging, similar to what can be obtained with Talbot-Lau interferometry.

Introduction

Neutron phase contrast imaging has followed a similar evolutionary path to that of X-ray phase contrast imaging (XPCI). As with X-rays, the interest in capturing the full complex refractive index is valuable to more fully characterizing a sample through new contrast mechanisms. Like X-rays, the real part of the refractive index for a material can be orders of magnitude different from the imaginary component. Unlike X-rays, where the value of the real part of the refractive index follows a general trend with atomic number, for neutrons, two materials that have similar imaginary components of the refractive index can have vastly different values for the real component[1]. This difference makes a compelling argument for developing techniques to measure the real component of the refractive index in neutron imaging. As in XPCI, there was quickly interest in moving away from the stringent requirements of crystal interferometers and crystal analyzer-based methods. Numerous facilities have now demonstrated the use of Talbot-Lau grating interferometers, a system employing two absorption gratings and a phase grating [1, 2]. In addition, a one-absorption, two-phase grating version called “far field” was recently tested

Sandia National Laboratories is a multimission laboratory managed and operated by National Technology & Engineering Solutions of Sandia, LLC, a wholly owned subsidiary of Honeywell International Inc., for the U.S. Department of Energy’s National Nuclear Security Administration under contract DE-NA0003525.

at NIST [3]. These systems are more neutron-efficient in that they work with larger neutron energy bandwidths and larger beam divergences. However, the fabrication of neutron gratings with the aspect ratios required continues to be a significant challenge. In this work we make the first demonstration with neutrons of a non-interferometric approach that uses two-absorption masks as first developed for X-ray imaging by Olivo and co-workers, which they coined "edge-illumination" [4]. In this preliminary experiment, the advantages noted are ease of optics fabrication and rapid setup. The disadvantages include inefficient use of neutron flux. The unknowns are sensitivity for phase contrast and scatter imaging and the optimal data processing scheme for a stepped-sample data acquisition mode. We have also observed the similarity between edge-illumination and the long-established field of structured illumination in the optical domain.

The physics governing the interactions between radiation and sample are well established [1, 5]. The new challenge is extracting and separating the attenuation, phase shift, and scatter information in the edge-illumination approach to neutron imaging in both the scenario of stepping the mask and that of stepping the sample.

For the purpose of comparing and contrasting edge-illumination with another grating-based experiment, Fig. 1 illustrates a Talbot-Lau interferometer with its wave propagation (black lines) and edge-illumination beamlets (blue arrows). When a low-resolution detector is used, the moiré fringe period is adjusted to be conveniently observable, spanning at least a few pixels or even larger than the full width of the detector. In the common case of several detected fringes, the data structure is analogous to fringe projection techniques used in structured illumination [6]. As we develop experience with edge-illumination, the data analysis tools to be evaluated will include Fourier analysis [7, 8], Levenberg-Marquardt fitting [9], vectorized least squares, Gaussian fitting [10], and the tools developed for structured illumination [6, 11]. In the present work, the vectorized least squares algorithm is used to process the stepped pre-sample mask data sets; the procedure for processing the stepped-sample data sets is still under development and should be able to model the signal from an extended object.

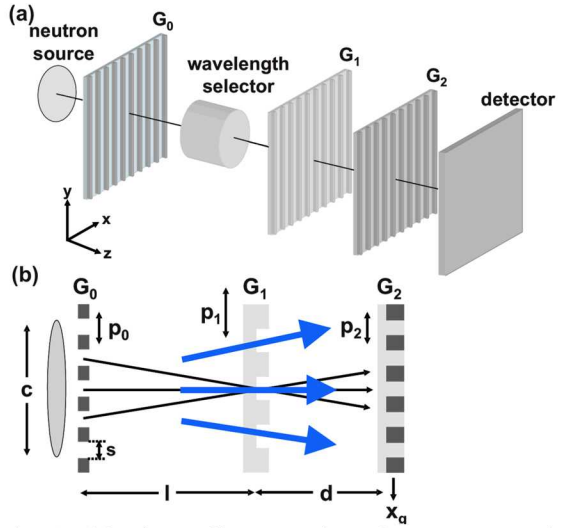

Fig. 1: (a) The Talbot-Lau interferometer. In the present work, G0 was replaced with a 1 mm slit, G1 a 182 μm period mask, and G2 a 200 μm period mask. (b) The black arrows show wave propagation in Talbot-Lau; the blue arrows represent the non-interfering beamlets of edge-illumination. (Figure adapted with permission from Review of Scientific Instruments, 79, (2008) 053703. Copyright 2008 AIP Publishing LLC).

The Talbot-Lau interferometer shown in Fig. 1 has small grating period dimensions leading to interference effects analogous to the Young's two-slit experiment. In the present work, edge-illumination uses masks with periods on the order of 200 μm. With such large periods, the interference effects between the beamlets drawn in blue (Fig. 1b) are negligible. The three masks form a structured illumination at the detector; the moiré pattern can be modulated by translation of a mask, typically the pre-sample mask.

Experiment

The edge-illumination imaging system was assembled at the ORNL CG-1D cold neutron imaging beamline. The beamline operates at the High Flux Isotope Reactor at a port viewing the liquid hydrogen moderator. The neutron beam was not monochromatic; wavelengths ranged from 0.8 to 6 Å with peak intensity at 2.6 Å. Between moderator and pinhole collimator (in this case, a slit), a supermirror neutron guide preserved intensity but added structure across the beam; a nanoparticle alumina diffuser reduced guide artifacts.

The distance between the 1 mm wide slit and the detector was 6 m. The last 0.5 m is shown in Fig. 2. The separation between the pre-sample mask (182 μm period) and the detector mask (200 μm period) was 0.5 m, determined by the beam divergence from the slit.

The ANDOR DW936 charge coupled device (CCD) camera was optically coupled to a 200 μm thick ^{6}LiF/ZnS scintillator, yielding a pixel size of 37 μm and an exposure time of 210 s; in the next experiment, the 1 mm slit will be replaced with a Lau mask (see Fig. 1) so as to reduce exposure time.

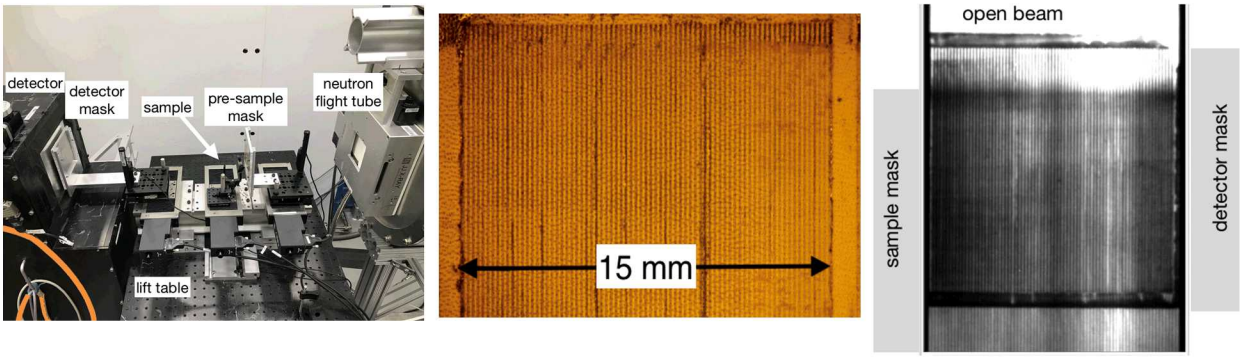

Fig. 2: (left) The edge-illumination setup showing the 0.5 m separation between the pre-sample mask and detector mask. (center) Optical image of the detector mask with 200 μm period; the absorber is Gd_2O_3 powder in 100 μm wide, 25 μm deep trenches milled in an aluminum plate. (right) Reference raw radiograph labeled with "open beam" and gray blocks showing vertical extents of pre-sample and detector masks.

The masks were fabricated with a Kern Evo micromill using 100 μm bits in 0.25" aluminum plate. The total depth of each trench was 50 μm and was milled in a single pass. Trenches with widths of 50 μm and 75 μm were attempted, but the mill bit breakage rate was excessive. The trenches were filled with Gd_2O_3 power, 5 μm particle size (Goodfellows). The powder was applied to the trenches as an ethanol slurry and spread with a single-edge razor blade. After drying, Kapton tape sealed the powder.

The masks were aligned with the beamline coordinate system by the HFIR Metrology Group using a Leica Absolute Tracker. In about 1 h, the metrologist aligned the three rotational settings for the two masks to the beamline axis system to within 0.5 mrad.

Data acquisition used two modes:

- Stepped Pre-Sample Mask: The pre-sample mask was translated by 10 μm increments over a range somewhat larger than the 182 μm mask period. Samples acquired over a single period tend to have a Gaussian shape, whereas samples acquired over more than a period tend to look sinusoidal due to the periodicity of the pre-sample mask. Stage accuracy is better than 1 μm. A reference image set was acquired just after mask alignment by the Metrology group, then used throughout the 36 h run. A sample data set required about 4 h; again, exposure time can be improved by replacing the 1 mm slit with a Lau mask. The

data were analyzed by fitting counts to sinusoids and to Gaussians with a scaling plus bias [10] for samples extending over a period, and a truncated set of samples, respectively.

- Stepped Sample: Here, the pre-sample mask was fixed in a position with a bright moiré fringe at the region of interest. Then, the sample was scanned by 10 μm increments over a range somewhat larger than the detector mask period of 200 μm. The data analysis procedure is still under discussion and should be able to model extended objects. One option has been fitting counts to an Erf(x) function, which can be interpreted as the spatial convolution of a Gaussian (characteristic curve over a grating period) with a unit step function (extended object) [10]; visual examination of that data supports this approach and may be easier to both process and interpret the parameters, compared to the sum of Gaussians model used by Olivo and co-workers [4].

Results

The edge-illumination setup was originally planned as a test setup for an upcoming Talbot-Lau interferometer to be installed at CG-1D. That is, the real goal was testing of mounts, stages, and software. The good performance of the edge-illumination method was a pleasant surprise.

The experimental performance is assessed based on the differential phase contrast and scattering sensitivities. For the scattering image, the results for a solid alumina (Al_2O_3) sphere are shown in Fig.3. The attenuation image shows vertical streaking which is attributed to an accidental shift of the step-up between measurement of the reference image set and the measurement of the sample images (data derived post-acquisition techniques can be used to improve the alignment of the sample positioning and will be discussed in a future paper). Otherwise, the attenuation image is routine. However, the scattering image shows very good scatter sensitivity. A test point from within the sample shows a good dynamic range in the amplitude of the sinusoidal signal between reference and sample data sets. First, the reference sinusoid shows visibility of over 30%, a value representative of the field of view. Second, the sample both attenuates and scatters. The scattering signal is calculated as

$$scattering(x,y) = \frac{amplitude_{sample}/offset_{sample}}{amplitude_{reference}/offset_{reference}}$$

$$scattering(110{,}200) = 39\%$$

A hollow aluminum sphere gave the best example of differential phase contrast imaging, Fig. 4. Nevertheless, the differential phase contrast shows the walls of the hollow aluminum sphere with alternating sign along the horizontal axis; the masks are aligned and translated so as to measure $d\Phi/dx$ (see coordinate system in Fig. 1).

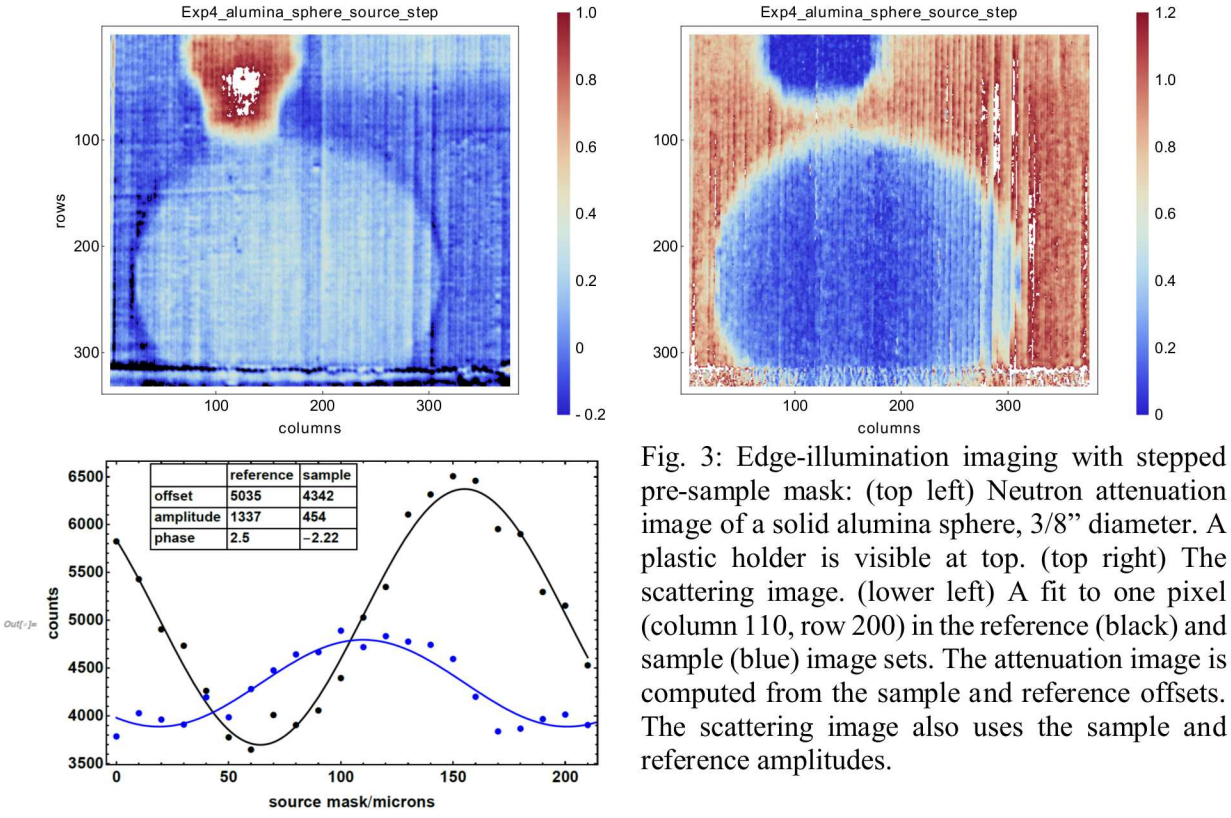

Fig. 3: Edge-illumination imaging with stepped pre-sample mask: (top left) Neutron attenuation image of a solid alumina sphere, 3/8" diameter. A plastic holder is visible at top. (top right) The scattering image. (lower left) A fit to one pixel (column 110, row 200) in the reference (black) and sample (blue) image sets. The attenuation image is computed from the sample and reference offsets. The scattering image also uses the sample and reference amplitudes.

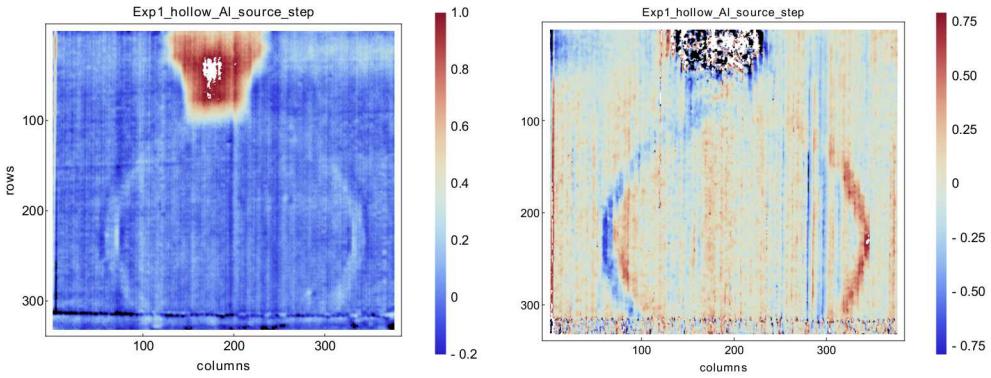

Fig. 4: Edge-illumination imaging with stepped pre-sample mask: (left) Neutron attenuation image of a hollow aluminum sphere, 3/8" diameter. (right) The differential phase contrast image showing the expected sign reversal at the edges.

Conclusions

At this writing, we can say that Talbot-Lau is the mature interferometry setup; far-field is of great interest due to the two-fold greater neutron efficiency; and edge-illumination (or structured illumination) is a fascinating, non-interferometric imaging system. The appeal lies in the potential ease of mask fabrication, thus allowing masks to be fabricated to match a sample's size and phase shift properties. In addition, edge-illumination is achromatic. And, edge-illumination shares the same alignment hardware as the interferometry setups. The data acquisition can employ either mask or sample translation. Olivo and co-workers have numerous publications on data analysis for the sample translation mode; efficient data analysis for this mode remains an area of research.

Acknowledgements
This material is based upon work supported by the US Department of Energy, Office of Science, Scientific User Facilities, under Contract DE-AC05-00OR22725 and was conducted at ORNL's High Flux Isotope Reactor, sponsored by the Scientific User Facilities Division, Office of Basic Energy Sciences, US Department of Energy.

Sandia National Laboratories is a multimission laboratory managed and operated by National Technology and Engineering Solutions of Sandia LLC, a wholly owned subsidiary of Honeywell International Inc. for the U.S. Department of Energy's National Nuclear Security Administration under contract DE-NA0003525.

The authors are thankful from contributions from Dr. Lowell Crow, the HFIR support groups, the HFIR Machine Shop, and Mrs. Lisa Fagan.

Micromilling expenses were funded through a DOE SBIR Phase I grant to Refined Imaging LLC.

References

[1] F. Pfeiffer, C. Grünzweig, O. Bunk, G. Frei, E. Lehmann, and C. David, "Neutron phase imaging and tomography," *Phys. Rev. Lett.*, vol. 96, no. 21, pp. 1–4, 2006.

[2] N. Kardjilov, I. Manke, A. Hilger, M. Strobl, and J. Banhart, "Neutron imaging in materials science," *Mater. Today*, vol. 14, no. 6, pp. 248–256, 2011.

[3] D. A. Pushin, D. Sarenac, D. S. Hussey, H. Miao, M. Arif, D. G. Cory, M. G. Huber, D. L. Jacobson, J. M. LaManna, J. D. Parker, T. Shinohara, W. Ueno, and H. Wen, "Far-field interference of a neutron white beam and the applications to noninvasive phase-contrast imaging," *Phys. Rev. A*, vol. 95, no. 4, pp. 1–7, 2017.

[4] M. Endrizzi, P. C. Diemoz, T. P. Millard, J. Louise Jones, R. D. Speller, I. K. Robinson, and A. Olivo, "Hard X-ray dark-field imaging with incoherent sample illumination," *Appl. Phys. Lett.*, vol. 104, no. 2, 2014.

[5] A. Momose, "Recent Advances in X-ray Phase Imaging," *Jpn. J. Appl. Phys.*, vol. 44, no. 9A, pp. 6355–6367, Sep. 2005.

[6] S. S. Gorthi and P. Rastogi, "Fringe projection techniques: Whither we are?," *Opt. Lasers Eng.*, vol. 48, no. 2, pp. 133–140, Feb. 2010.

[7] C. Grünzweig, F. Pfeiffer, O. Bunk, T. Donath, G. Kühne, G. Frei, M. Dierolf, and C. David, "Design, fabrication, and characterization of diffraction gratings for neutron phase contrast imaging," *Rev. Sci. Instrum.*, vol. 79, no. 5, pp. 1–6, 2008.

[8] E. E. Bennett, R. Kopace, A. F. Stein, and H. Wen, "A grating-based single-shot x-ray phase contrast and diffraction method for in vivo imaging," *Med. Phys.*, vol. 37, no. 11, pp. 6047–6054, 2010.

[9] N. Kardjilov, I. Manke, R. Woracek, A. Hilger, and J. Banhart, "Advances in neutron imaging," *Mater. Today*, vol. 21, no. 6, pp. 652–672, 2018.

[10] M. Endrizzi and A. Olivo, "Absorption, refraction and scattering retrieval with an edge-illumination-based imaging setup," *J. Phys. D. Appl. Phys.*, vol. 47, p. 505102, 2014.

[11] C. J. Maughan Jones, F. A. Vittoria, A. Olivo, M. Endrizzi, and P. R. T. Munro, "Retrieval of weak x-ray scattering using edge illumination," *Opt. Lett.*, vol. 43, no. 16, p. 3874, 2018.